Hindawi
Wireless Communications and Mobile Computing
Volume 2022, Article ID 6548800, 16 pages
https://doi.org/10.1155/2022/6548800

Research Article

Prediction of Wear Rates of UHMWPE Bearing in Hip Joint Prosthesis with Support Vector Model and Grey Wolf Optimization

Rania E. Hammam,[1] **Hani Attar**,[2] **Ayman Amer**,[2] **Haitham Issa**,[3] **Ioannis Vourganas**,[4] **Ahmed Solyman**,[5] **P. Venu**,[6] **Mohammad R. Khosravi**,[7] **and Mohanad A. Deif**[1]

[1]*Department of Bioelectronics, Modern University of Technology and Information (MTI) University, Egypt*
[2]*Department of Energy Engineering, Zarqa University, Jordan*
[3]*Department of Electrical Engineering, Zarqa University, Jordan*
[4]*School of Design and Informatic, Abertay University, UK*
[5]*Department of Electrical and Electronics Engineering, Istanbul Gelisim University, 34310 Avcılar, Turkey*
[6]*Department of Mechanical Engineering, College of Engineering, University of Bahrain, Bahrain*
[7]*Department of Computer Engineering, Persian Gulf University, Bushehr, Iran*

Correspondence should be addressed to Mohammad R. Khosravi; m.khosravi@mehr.pgu.ac.ir

Received 19 January 2022; Revised 11 April 2022; Accepted 19 April 2022; Published 9 May 2022

Academic Editor: Xin Ning

One of the greatest challenges in joint arthroplasty is to enhance the wear resistance of ultrahigh molecular weight polyethylene (UHMWPE), which is one of the most successful polymers as acetabular bearings for total hip joint prosthesis. In order to improve UHMWPE wear rates, it is necessary to develop efficient methods to predict its wear rates in various conditions and therefore help in improving its wear resistance, mechanical properties, and increasing its life span inside the body. This article presents a support vector machine using a grey wolf optimizer (SVM-GWO) hybrid regression model to predict the wear rates of UHMWPE based on published polyethylene data from pin on disc (PoD) wear experiments typically performed in the field of prosthetic hip implants. The dataset was an aggregate of 29 different PoD UHMWPE datasets collected from Google Scholar and PubMed databases, and it consisted of 129 data points. Shapley additive explanations (SHAP) values were used to interpret the presented model to identify the most important and decisive parameters that affect the wear rates of UHMWPE and, therefore, predict its wear behavior inside the body under different conditions. The results revealed that radiation doses had the highest impact on the model's prediction, where high values of radiation doses had a negative impact on the model output. The pronounced effect of irradiation doses and surface roughness on the wear rates of polyethylene was clear in the results when average disc surface roughness (R_a) values were below 0.05 μm, and irradiation doses were above 95 kGy produced 0 mg/MC wear rate. The proposed model proved to be a reliable and robust model for the prediction of wear rates and prioritizing factors that most significantly affect its wear rates. The proposed model can help material engineers to further design polyethylene acetabular linings via improving the wear resistance and minimizing the necessity for wear experiments.

1. Introduction

The hip joint is one of the most important synovial joints in the human body; so, when it is arthritic or injured, the natural hip joint must be replaced to relieve the related discomfort and to reestablish its functionality. Consequently, the acetabular cartilage and femoral surfaces are removed and then replaced by a hemispherical acetabular component and a spherical femoral head to complete the joint replacement process successfully [1].

Since artificial joints functions under sliding and rolling situations [2, 3], particular mechanical wear validation

processes are performed over it to testify the replacement joint's specifications, such as adhesion, abrasion, and fatigue. The adopted verification processes is called 'the surface degradation validation,' taking into consideration that increasing the external load and/or the surface roughness of the replacement joint's contact materials speeds up the wear process. The tribiological system of the joint prosthesis and its deterioration process is defined by the interplay of all of these elements. Consequently, the mechanical qualities and wear resistance of the typical artificial joint's component materials dictate its expected lifetime.

Metallic alloys, including ceramics or cobalt-chromium-molybdenum alloys (CoCrMo), such as alumina composites, agreed to have good functional characteristics, such as hardness, chemical stability, and wear resistance, which allows employing them for the femoral bearings [4].

Ultrahigh molecular weight polyethylene (UHMWPE) is also regarded as one of the most successful acetabular bearing materials in total hip prosthesis due to its inimitable mixture of superior wear, fatigue resistance, toughness, chemical stability, as well as a good biocompatibility over other polymers [5, 6]. However, nowadays, UHMWPE produces nanosized and submicron wear debris in large amounts, overwhelming the body's capability to effectively remove the material. The generated wear debris triggers hostile tissue reactions while articulating with the metallic contact, which leads to osteolysis or bone loss followed by implant loosening and failure [7–9]. The major problem that limits the lifetime of the complete joint prosthesis is the related polyethylene wear-induced osteolysis.

Thus, intensified investigations were conducted on increasing the performance and UHMWPE wear resistance in the last 50 years, to provide patients who are youthful and active with long-lasting and effective implants. The studies included methods for enhancing the properties of UHMWPE, such as cross-linking through irradiation [10], surface modification through plasma treatment [11, 12], or reinforcements with particles or fibers [13–15].

Recently, cross-linked ultrahigh molecular weight polyethylene has been developed for the use of acetabular cups of hip joint prostheses. A major advantage of cross-linked UHMWPE is that it has lower wear rates compared to the conventional uncross-linked material. Among all cross-linking procedures, Irradiation is the most popular and successful process for cross-linking and/or sterilizing UHMWPE [16–19]. Radiation cross-linking developed by the use of high doses of gamma or electron beam radiation was reported to improve the hardness, lower the ductility of the polymer, and enhance the UHMWPE wear resistance [19–21]. This is because the presence of cross-links prevents UHMWPE from orienting on its surface and thus decreases the production of wear particles caused by shear forces from crossing path motion [22].

UHMWPE wear resistance improves when the radiation does increases; however, high dose rates of radiation accelerate the oxidation process as a result of the presence of free radicals that react with oxygen causing brittleness and failure of the implant [23]. Consequently, efforts have been undertaken to reduce the free radicals via thermal treatment, such as gamma-irradiated and melted UHMWPE [24], gamma-irradiated and annealed UHMWPE [25], and vitamin-E blending in UHMWPE as a free radical scavenger. Highly cross-linked polyethylene (HXPE) and vitamin-E-infused/blended cross-linked polyethylene (VEXPE) have shown substantially less wear in vitro [26] and in vivo [27] than the ordinary UHMWPE.

To assess the wear behavior of UHMWPE utilized in metal-on-polyethylene (MoP) prosthetic hip implants, several testing configurations such as pin-on-disc (PoD), pin-on-plate, and hip joint simulators have been employed. In a PoD wear measurement coupled to MOP prosthetic hip implants, a polyethylene pin is loaded against a metallic disc, and relative motion between the pin and the disc causes polyethylene wear. PoD wear studies are frequently performed to quantify, compare, and rank the wear of various implant-bearing material combinations as a function of operational factors and environmental conditions. Comparing polyethylene wear results from numerous PoD tests, on the other hand, might be time consuming and complex, potentially leaving information unclear.

However, in recent years, researchers have employed machine learning techniques in conjunction with existing datasets to facilitate modeling complex correlations between material structure, constituents, and the corresponding mechanical qualities. These models also help in visualizing and comparing datasets, as well as predicting new results based on the existing knowledge embedded in the model, which would otherwise be difficult or time-consuming to obtain using traditional experimental methods [28].

Intelligent prediction and analysis models have been introduced and studied by many researchers in various applications. Gated recurrent unit (GRU) networks have been proposed for point of interest (PoI) category prediction [29] and next PoI recommendation [29]. A long short-term memory (LSTM) model has been studied by Liu et al. [30] for green house climate prediction. Abbasi and Rafiee [31] presented a new analysis framework for predicting the performance of packet classification algorithms on GPU-like highly threaded machines. Nowadays, the internet of things (IoT) has attracted many researchers and academics due to its innovative functions and applications in many fields, such as smart city applications [32] and intelligent transportation systems [33].

Due to the complex wear behavior of UHMWPE, it is necessary to find a practical machine learning model to predict the wear rates of polyethylene and therefore supplement time consuming PoD experiments. Hence, this study was aimed at proposing an efficient machine learning algorithm that predicts the wear rates of UHMWPE applied as a bearing material in hip joint prosthesis. The employed dataset was based on published polyethylene data from PoD wear experiments specifically performed in the field of prosthetic hip implants. The proposed model facilitates the understanding and comparison of the data driven from PoD experiments in order to predict the wear performance of UHMWPE inside the body and, therefore, predict its lifetime, which also helps material engineers to further improve the design of polyethylene acetabular linings in order to

enhance its performance and mechanical properties and lengthen its lifetime inside the body. The model also assists in identifying and prioritizing factors that most significantly affect polyethylene wear rates. A correlation between the different parameters and wear rates of UHMWPE was also investigated. Another important goal of the proposed research is to investigate the impact of radiation doses and their relation to other factors affecting the wear rates of polyethylene, which helps in determining the optimum radiation doses that produce lower wear rates.

The proposed machine learning models presented in this work were Classic SVM, SVM-GWO, SVM using practical swarm optimizer (SVM-PSO), SVM using the genetic algorithm optimizer (SVM-GA). The model's performance was assessed using the root mean square error (RMSE) and the R^2 scores to select the best fit model capable of analyzing and predicting the UHMWPE wear rates based on several operating parameters in PoD experiments. Furthermore, Shapley additive explanations (SHAP) values were used to interpret the model's prediction accuracy.

2. Materials and Methods

2.1. Dataset Acquisition. The dataset employed in the proposed study consisted of 129 data points and is adapted from a previous work conducted by Borjali et al. [34]. The dataset was an aggregate of 29 different PoD published UHMWPE datasets performed in the field of prosthetic hip implants. Published datasets collected from Google Scholar and PubMed databases were gathered using keywords including "UHMWPE", "wear", "hip" and "Pin-on-Disc". CoCrMo alloys and ceramics are the two most popular materials for the femoral head in hip joint prostheses, while the acetabular liner is often constructed of ultrahigh molecular weight polyethylene, as discussed earlier in this paper. As a result, this study focused solely on multidirectional motion between a polyethylene pin and a CoCr disc, with flat-on-flat geometry and bovine serum as a lubricant.

Additionally, only experiments with properly specified and published operating input parameters as well as polyethylene wear rate statistics were included. UHMWPE wear was assessed using the ASTM F732 standards wear rate (mg/MC), which is measured in terms of material loss per million cycles (MC). The wear rate is calculated by multiplying the normal load, sliding distance, and polyethylene density by the wear factor, which is the wear volume per normal load unit and sliding distance [35]. In cases of missing polyethylene densities, a UHMWPE density of 0.93 mg/mm^3 was employed, as reported in previous literature [36]. The UHMWPE materials employed in the dataset were mostly conventional GUR 1020 and 1050. The lubricant temperature range was 25-37°C.

2.2. Input Parameters. Several important parameters have a major impact on the UHMWPE wear rates in PoD experiments and, therefore, affect its performance in vivo when applied to the acetabular lining in the hip joint prosthesis. Polyethylene wear has been linked to both the applied stress on the pin and the contact area between the pin and the disc by several researchers [37, 38]. The UHMWPE wear rate is also affected by the disc surface roughness [39] and the lubricant employed in the PoD wear tests. Bovine serum is frequently utilized as a lubricant for PoD wear trials in the setting of prosthetic hip implants [40].

The wear aspect ratios and sliding distances are also relevant factors affecting the wear rates of polyethylene. The wear aspect ratio is a metric for determining the shape of motion paths and, as a result, the likelihood of wear between the femoral head and the polyethylene acetabular cup liner. The sliding distance is the overall length of the worn path. The radiation dose (presented in [41]) is another major aspect mentioned in the literature; increasing the radiation dose enhances polyethylene cross-linking, which increases wear resistance.

The shapes of the multidirectional wear path employed in the dataset were rectangular, elliptical, circular, and square paths. In the circular and elliptical wear pathways, cross-shear occurs on the surface of the pin throughout the worn route, whereas cross-shear occurs when the pin changes direction along the worn path in the rectangular and square wear paths.

Hence, the most relevant operating factors affecting the wear rates of UHMWPE in PoD experiments were selected as input parameters to the proposed models. These parameters included the following: contact area (mm^2), wear path aspect ratio, normal load (N), sliding distance per cycle (mm/C), disc average surface roughness (R_a) (μm), polyethylene radiation dose (kGy), frequency (HZ), and test duration in million cycles (MC). The description of the input operating parameters is summarized in Table 1.

2.3. Preliminaries

2.3.1. Support Vector Machine (SVM). SVM is a machine learning model that is commonly employed. It is typically suited for small sample sizes and has a strong statistical base [42–44]. In the disciplines of energy, ecology, hydrology, and economics, SVM has numerous applications [45, 46]. In a regression issue, the training set is defined as [46–48]

$$\left\{\left(x_j, y_j\right) \middle| x_j, y_j \in R^n, j = 1, 2, \cdots n\right\}, \tag{1}$$

where x_j and y_j are the input and the output, respectively. The SVM model's detailed form is

$$f(x) = \varpi^T \phi(x) + c, \tag{2}$$

where ϖ and $\phi(x)$ are the weighted vector and the nonlinear mapping function, respectively, and c is the deviator. In the SVM model, the two hyperparameters that influence prediction performance are the kernel width and the penalty factor.

2.3.2. Multiobjective Grey Wolf Optimizer. The GWO [49, 50] is the foundation for building a multiobjective GWO. The GWO algorithm is a metaheuristic algorithm based on wolf hunting behavior. Every wolf in the herd has the potential to be a solution to the problem. The ideal, suboptimal,

Table 1: Input parameters.

Parameter	Description
Contact area	Contact area between the polyethylene pin and the CoCr disc which in vivo represents the contact area between the CoCr femoral head and UHMWPE acetabular liner in the hip joint prosthesis and it is measured in mm^2
Wear path aspect ratio	The ratio of the wear path length to the perpendicular width of path, and it provides a way to quantify the shape of motion paths
Normal load	Applied stress on the polyethylene pin and it is measured in Newton which clinically represents the weight of the patient on the artificial hip prosthesis
Sliding distance per cycle	Overall distance of the worn path taken by the polyethylene pin in PoD experiments and it is measured in mm per cycle
Disc average surface roughness (R_a)	Surface roughness is calculated measuring the average of surface heights and depths across the surface. (R_a) is the arithmetic average of the absolute values of the profile height deviations from the mean line, recorded within the evaluation length. This value summarizes the roughness level of the polyethylene disc employed in PoD experiments. It is measured in micrometer (μm)
Polyethylene radiation dose	Radiation dose in (kGy) which indicates the level of cross-linking in polyethylene and therefore enhanced wear resistance
Frequency	Number of cycles per second and measured in Hz. The frequency included in the dataset was around (1.8 Hz) in order to simulate human gait frequency
Test duration	Duration of test in MC

and alternate solutions are represented by the four levels of the wolf swarm. Wolves approach their prey when they find it. Its position equations are

$$\begin{cases} \vec{J} = \left| \vec{M} \cdot \overrightarrow{L_p}(p) - \overrightarrow{L_w}(p) \right|, \\ \overrightarrow{L_w}(p+1) = \overrightarrow{L_p}(p) - \vec{N} \cdot \vec{J}, \end{cases} \tag{3}$$

where the separation distance between the prey and the wolf is given by $\vec{J}$, $\vec{M}$, and $\vec{N}$ are coefficient vectors, the position vectors of the grey wolf and the prey are $\overrightarrow{L_w}$ and $\overrightarrow{L_p}$, and the current iteration is given by p.

GWO saves the top three solutions and uses Equations (4) and (5) to identify the optimum solution and continuously updates the position of the grey wolf:

$$\begin{cases} \overrightarrow{J_\alpha} = \left| \overrightarrow{M_1} \cdot \overrightarrow{L_\alpha}(p) - \overrightarrow{L_w}(p) \right|, \\ \overrightarrow{J_\beta} = \left| \overrightarrow{M_2} \cdot \overrightarrow{L_\beta(p) - L_w(p)} \right|, \\ \overrightarrow{J_\gamma} = \left| \overrightarrow{M_3} \cdot \overrightarrow{L_\gamma}(p) - \overrightarrow{L_w}(p) \right|, \\ \overrightarrow{L_1} = \overrightarrow{L_\alpha}(p) - \overrightarrow{N_1 J_\alpha}, \\ \overrightarrow{L_2} = \overrightarrow{L_\beta(p) - N_2 J_\beta}, \\ \overrightarrow{L_3} = \overrightarrow{L_\gamma}(p) - \overrightarrow{N_3 J_\gamma}, \end{cases} \tag{4}$$

$$\overrightarrow{L_p}(p+1) = \frac{1}{3}\left(\overrightarrow{L_1} + \overrightarrow{L_2} + \overrightarrow{L_3}\right), \tag{5}$$

where α, β, and γ are different levels of grey wolves.

The newly created individual is compared to the archived individual after each iteration. Furthermore, all individuals are categorized depending on the distance of the objective function value to avoid an overabundance of similar individuals. The problem of directly selecting three nondominant solutions using the Pareto technique [51] was overcome by using a roulette to choose the archive's leader wolf. Equation (6) can calculate the probability of each hypercube [52].

$$P_i = L_i^{-c}, \tag{6}$$

where P_i is the probability of the hypercube, L_i is the number of Pareto optimal solutions, and c is a constant.

2.4. Shapley Values. The SHAP technique is based on the Shapley value principle from the game theory [53, 54]. The Shapley value (SHAP) principle was developed to anticipate the relevance of an individual player in a cooperative team. This concept is based on the relative importance of each player's participation to the game's outcome and is meant to distribute the total profit or payment among them. Shapley values produce a distinct result that is distinguished by the following natural features or axioms: consistency (symmetric), local accuracy (additivity), and nonexistence (null effect) [43, 55–57], which offer a solution to each player's problem of allocating a fair or appropriate reward.

Shapley values take into consideration elements of varying magnitudes and signs that contribute to the model's prediction or forecast. As a result, Shapley values are estimates of the function's importance (amount of contribution) as well as its direction (sign). Positive SHAP values indicate an increase in the wear rates of polyethylene, whereas negative SHAP values indicate a decrease in the wear rates. The features in the proposed study represent the input operating parameters affecting the wear rates of UHMWPE in PoD experiments. Specifically, the feature i significance is defined by the Shapley value in

$$\varnothing_i = \frac{1}{|N|!} \sum_{SCN\setminus\{i\}} |S|!(|N| - |S| - 1)![f(S \cup \{i\} - f(S))], \quad (7)$$

where $f(S)$ relates to the model output, which can be clarified by the S set of features, and the entire set of all features N. The ultimate impact of the Shapley value of feature $i\varnothing_i$ is determined as the middling of its contributions across all possible feature set permutations. Features are then individually applied to the collection, and their importance is exposed by the shift in model performance. Importantly, this approach takes into account feature orderings, which influence reported changes in a model's performance in the presence of correlated information.

2.5. Proposed Approach. The prediction system includes three phases as shown in Figure 1: (1) data preprocessing, (2) developing an optimization and prediction system, (3) performance analysis, and (4) interpreting the best fit model using SHAP value.

2.5.1. Data Preprocessing. The main purpose of this step removes the artifacts from the dataset (variables that have missing data points and outlier data) to improve prediction system performance. After that, the dataset was split into two parts. One part is used for training the regression models, while the other part is used for the final evaluation of the models.

2.5.2. Development of the Regression Algorithm. After the preprocessing is complete, the processed data is entered into the SVM-GWO hybrid regression system. This model consists of two operations (training and optimization of the regression model). In the training set, these two procedures are synchronized and executed. That is, both SVM training and optimization are carried out simultaneously. When the optimization is complete, the SVM training is also completed. Academics often create an objective function to reduce the training set's prediction error in the traditional optimization problem (single-objective optimization). Since the multiobjective optimization used in this article takes into consideration both the precision and the stability of the prediction, two objective functions are defined as

$$m = \begin{cases} \text{Obj}_{\text{Acc}} = \text{RMSE}_{\text{training}} = \dfrac{1}{S_t} \displaystyle\sum_{k}^{S_t} \left| \frac{A_k - P_k}{A_k} \right|, \\ \text{Obj}_{\text{St}} = \text{std}(A_k - P_k), \end{cases} \quad (8)$$

where Obj_{St} and Obj_{Acc} are the objective stability and prediction precision functions, respectively, $\text{RMSE}_{\text{training}}$ is the training set RMSE, S_t is the training set's sample size, A_k and P_k are the actual and at time k predicted values, and std is the population's standard deviation. Algorithm 1 lists the SVM-GWO global hybrid regression system pseudocode.

In the proposed paper, GWO has been used among other optimization algorithms because the advantages of GWO are as follows: easy to implement due to its simple structure, less storage and computation requirements, faster convergence due to continuous reduction of search space, fewer decision variables, and the ability to avoid local minimums with only two control parameters to adjust the performance of the algorithm, which ensure better stability and avoid complexity.

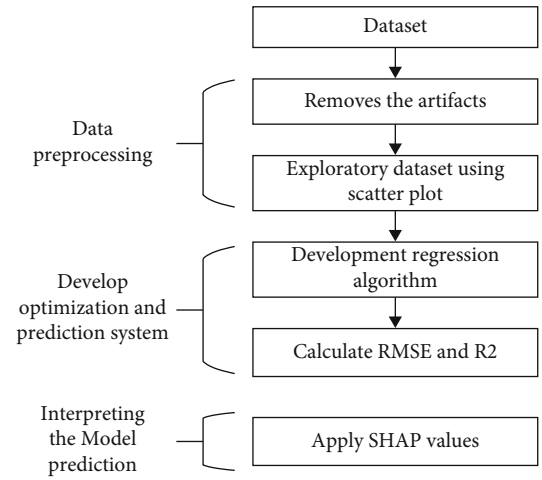

Figure 1: Overall methodology steps.

To emphasize the benefits of the proposed model, this paper defines three models as the benchmark models for comparison with our proposed method. The first one of these models is the classic SVM model, and the second and third models are the SVM-PSO and using the genetic algorithm optimizer (SVM-GA). The theory of the benchmark models as well as the reasons for selecting them are previously reported in reference [58].

2.6. Model Evaluation. Commonly used metrics are employed in the proposed study to evaluate the performance and prediction errors of the proposed models. These metrics include the square of the correlation coefficient R^2 [59, 60] and the RMSE [61]. The values of both metrics yield a good indication of the accuracy and prediction capability of the proposed models and allow us to select the most efficient model for the prediction of wear rates of UHMWPE.

RMSE is computed as

$$\text{RMSE} = \sqrt{\frac{\sum_{i=1}^{n} (a_i - p_i)^2}{n}}, \quad (9)$$

where a_i is the actual value, p_i is the predicted value of the i^{th} data point, and n is the dataset's total number of data points.

The value of R^2 is calculated as

$$R^2 = 1 - \frac{\sum_{i=1}^{n} (a_i - p_i)^2}{\sum_{i=1}^{n} (a_i - a)^2}. \quad (10)$$

2.7. Using the SHAP Values to Interpret the Model Prediction. In the proposed work, the SHAP technique was employed to understand the importance of the several parameters that affect the model's prediction of the wear rates of UHMWPE and therefore help in predicting its

Algorithm: SVM-GWO
Inputs: parameters of SVM and GWO (wolf number (x), dimension number (y), search domain (z)), dataset_ records[forecast dataset]
Output: value of (wear rates of UHMWPE)
1: ***Initialization of variables:***
Set*x* ⟵*random (1, 1)*
Set*y* ⟵*random (1, 1)*
Set*z* ⟵*random (1, 1)*
2: ***Initialize training procedure:***
Set *iterations* ⟵ *i*
3: ***for each*** *iteration* ***in*** *iterations:*
SVM *(dataset_records[iteration][all], x, y, z)*
End
4: ***Calculate fitness function:***
Set*l* ⟵***get_length****(dataset_records)*
Set fitness_array *[]*⟵***zeros*** *(1, l)*
5: ***for counter in range*** *(l):*
fitness_array[]⟵ ***fitness.calculate(dataset_records)***
End
6: ***find*** *non_dominant_solution*
7: ***initialize*** *archive*
8: ***for each*** *iteration* ***in range****(iterations):*
if (true):
Output: *SVM with hyperparameters*
else:
search_agent.position ⟵ *iteration*
Fitness_array[]⟵*fitness.calculate(:)*
Update: *non_dominant_solution*
Update: *archive*
End
End
9: ***for each****N* ***in range(length****(archive)):*
if (true):
pareto_archive_member.remove()
else:
return: *SVM.hyperparamteres.optimal()*
output: *SVM.hyperparameters.optimal()*
End
End

Algorithm 1: Hybrid regression system in pseudocode.

in vivo wear performance. Prioritizing factors that affect the UHMWPE wear performance in hip joint prosthesis can assist material engineers to further improve the design of polyethylene acetabular linings and hence improve its wear resistance and expand its lifetime inside the body. A main benefit of the associated SHAP values is that they add interpretability to complicated models. The model interpretability was evaluated both locally and globally by looking at the relative importance of the variables and their impact on the model's prediction. Global interpretability helps to understand the entire structure of the model, and it can be obtained through summary plots and bar plots that demonstrate the significance of the overall features. The SHAP summary map depicts how much each predictor contributes to the target outcome variable (wear rates of UHMWPE) either positively or negatively. Features are organized by the sum of the magnitudes of the SHAP values in all the samples, i.e., by their global impact $\sum_{j=1}^{N}|\varnothing_i^{(j)}|$. SHAP values $\varnothing_i^{(j)}$ are drawn horizontally.

Table 2: Evaluation metrics of the proposed models.

Model name	RMSE	R^2
Classic SVM	3.304	0.84
SVM-PSO	3.374	0.91
SVM-GA	2.828	0.88
SVM-GWO	2.345	0.96

3. Results and Discussion

The primary target of this study is to develop a model having the highest efficiency and capability of predicting the UHMWPE wear rates based on cross-path motion in the hip joint prosthesis. Cross-shear occurs when the relative motion between the pin and the disc changes direction with regard to the surface of the pin, preventing polymer molecular alignment and resulting in polyethylene wear similar to that found in vivo. It was reported that a combination of multidirectional and a serum-based lubricant is known to be essential requirements for laboratory simulation of clinical wear mechanisms of prosthetic hip joints [21, 62]; therefore, PoD wear experiments employing Bovine serum as lubricants are included in this work.

To select the most efficient model, the performance of the implemented models was evaluated using RMSE and R^2 scores, and their values were tabulated in Table 2.

It was clear from Algorithm 1 that the SVM-GWO outperformed the other implemented models since it attained the least RMSE and the highest R^2 score for prediction of the UHMWPE wear rates. It is known that if the RMSE approaches zero, the model's performance is regarded as being excellent [63]. As a result, the suggested model's SVM-GWO RMSE value of 2.345 indicates that the model's predicted values are inconsistent with the experimental data, and all errors are within acceptable limits. Furthermore, the R^2 score having a value of 0.96, which is very close to 1, tells us that all points predicted by the model lie exactly on the experimental or actual data curve with no scatter and the results have the perfect correlation. Since the results showed the high accuracy and reliability of SVM-GWO as compared to the other counterpart models, it was further employed in this study to analyze and predict the UHMWPE wear rates based on different operating parameters.

To interpret the SVM-GWO and to show the relative importance of the different variables (input operating parameters) on the predicted wear rates of UHMWPE, an aggregate bar graph was performed and shown in Figure 2. The bar graph plots the mean absolute SHAP value for each variable. Moreover, a SHAP summary plot shown in Figure 3 was developed that provided more context than the bar chart and also their range of effects over the dataset. A row of the dataset is represented by each point in the SHAP summary plot. This is similar to a bar plot, except it can illustrate if each variable has a negative or positive

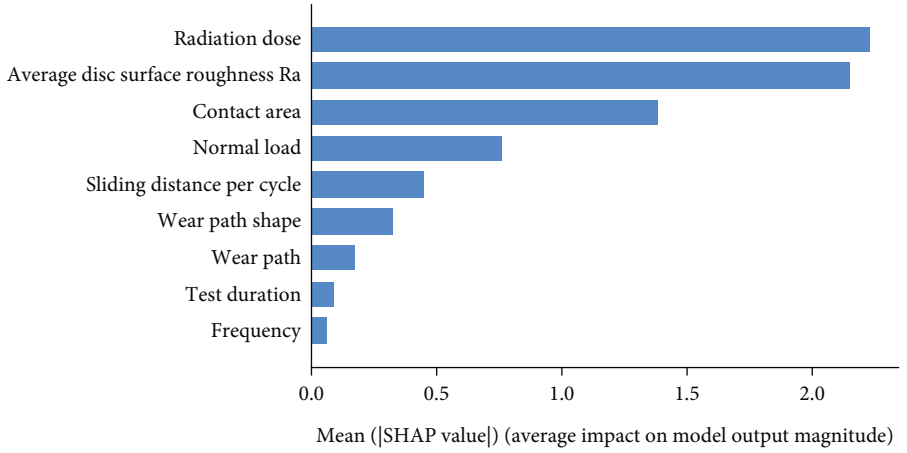

Figure 2: Bar plot to show the importance of each feature.

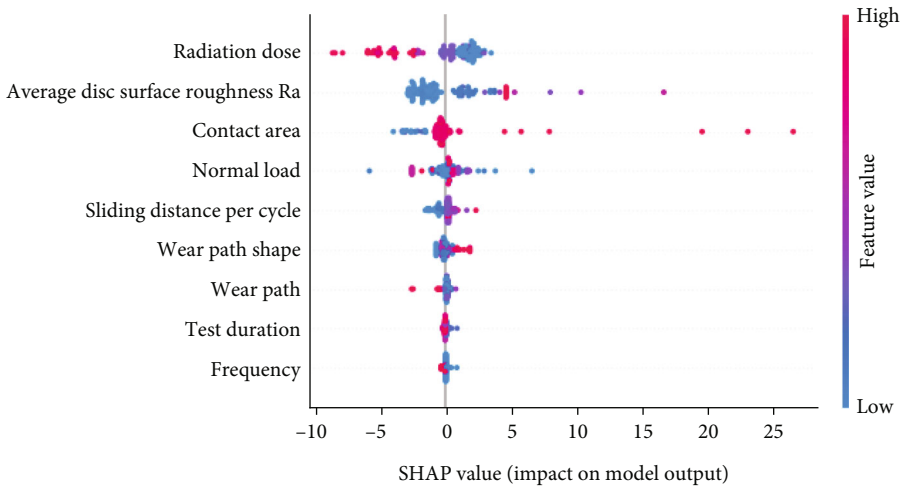

Figure 3: Model 2 summary plot for SHAP.

relationship with the output target. The significance of the features is ranked in ascending order. In the SHAP summary plot, the horizontal location indicates whether the influence of that value is associated with a higher or lower model prediction. The x-axis points indicate the impact on the model output and whether it is positive or negative. Color refers to either high (red) or low (blue) relative variables. Positive SHAP values indicate an increase in the wear rates of UHMWPE, whereas negative SHAP values indicate a decrease in the wear rates predicted by the model.

It was seen from the bar plot in Figure 2 that the parameters having a major effect on the prediction models of UHMWPE wear rates are ranked as follows from the most important to the least: radiation dose, average disc surface roughness, contact area, normal load, sliding distance, and wear path shape.

The SHAP summary plot in Figure 3 revealed that the radiation doses had the maximum impact on the model's prediction, where high values of radiation doses had a negative impact on the model output wear rate of UHMWPE implying that high doses of radiation decrease the wear rate of UHMWPE, which is similar to previous findings since irradiation increases the cross-linking in polyethylene which in turn improves its wear resistance. The second significant parameter is the disc surface roughness. However, it is not clear from the curve whether low values affect positively or negatively on the model output. Another relevant observation from the SHAP summary plot is that high values of contact area affect positively the model's prediction, which tells us that as the contact area increases, it leads to an increase of polyethylene wear rates, which is compatible with clinical results, which is because in vivo, the metal on plastic prosthetic hip implants show increasing wear rates with increasing femoral head size which means that large contact areas between femoral head and UHMWPE liner increases the wear rate of UHMWPE liner. Because the dataset covers a short range (1.8 Hz) to simulate human gait frequency, the influence of frequency on polyethylene wear rates had no evident effect on the model's prediction.

To get a deeper understanding of the interactions between different operating parameters, SHAP dependence plots were further developed. They depict the marginal effect

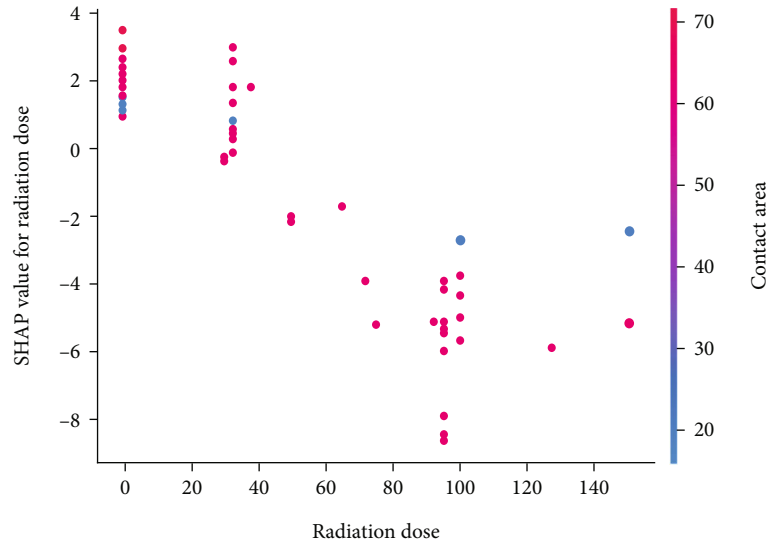

(a)

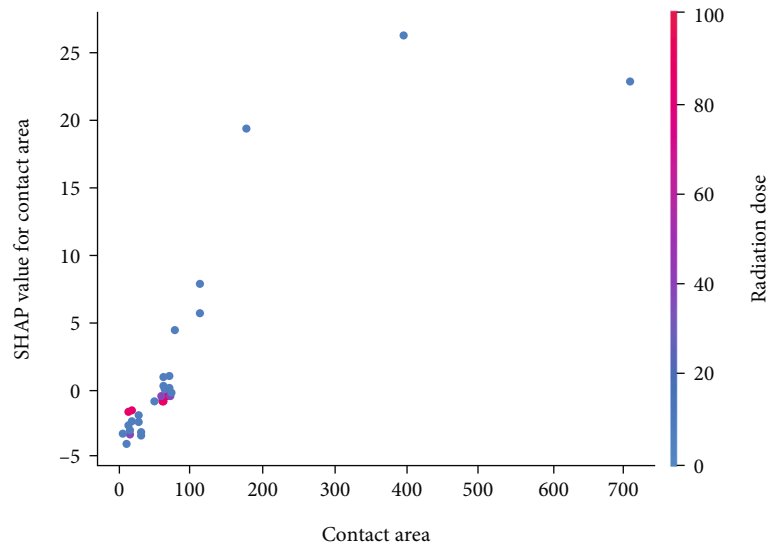

(b)

Figure 4: Continued.

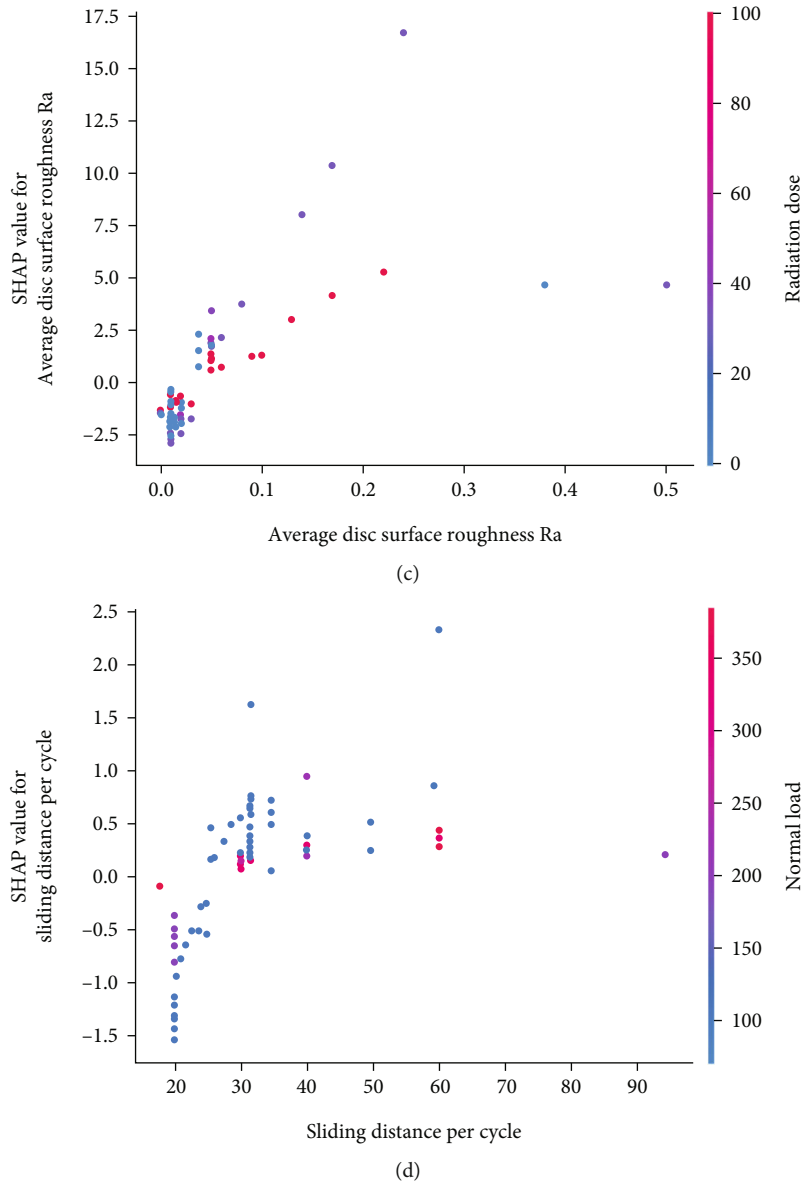

Figure 4: (a) Dependence plot that shows SHAP values of radiation dose. (b) Dependence plot that shows SHAP values of contact area. (c). Dependence plot that shows SHAP values of average disc roughness. (d) Dependence plot that shows SHAP values of sliding distance.

that one or two variables have on the predicted outcome of the model. Each dot represents a single row from the dataset. The value of the feature appears on the x-axis and the y-axis is the SHAP value for that feature, which defines how much the feature's value affects the model output. The color relates to a second feature that may have a combined effect with the feature that has been plotted. The second feature is selected automatically. Figure 4 shows dependence plots between different input parameters and their effect on the model predicted outcome. Figure 4(a) shows the SHAP values of radiation doses, and the contact area was selected to show the interaction between them. It was clear that there were three ranges of radiation doses in the dataset, 0 kGy (nonirradiated polyethylene), 30-50 kGy (conventional polyethylene), and 95-150 kGy highly cross-linked UHMWPE-HXPE. It was noticed that nonirradiated polyethylene (0 kGy) accompanied with large contact areas had the highest wear rates since it showed positive SHAP values. On the other hand, high values of radiation doses higher than 95 kGy accompanied by large contact areas produced the lowest wear rates of UHMWPE since it showed the lowest prediction of the model (negative SHAP values). This conclusion was in agreement with a previous study [64] which employed different wear settings in PoD experiments but the authors also reported that radiation doses of 100 kGy increased the cross-linking density of UHMWPE and thus its wear resistance.

Figure 4(b) showed that there was a positive trend between the contact area and the target variable (wear rate). The higher the values of contact areas, the more positive the SHAP values, which means higher wear rates which is compatible with clinical results [64]. In addition, low values of

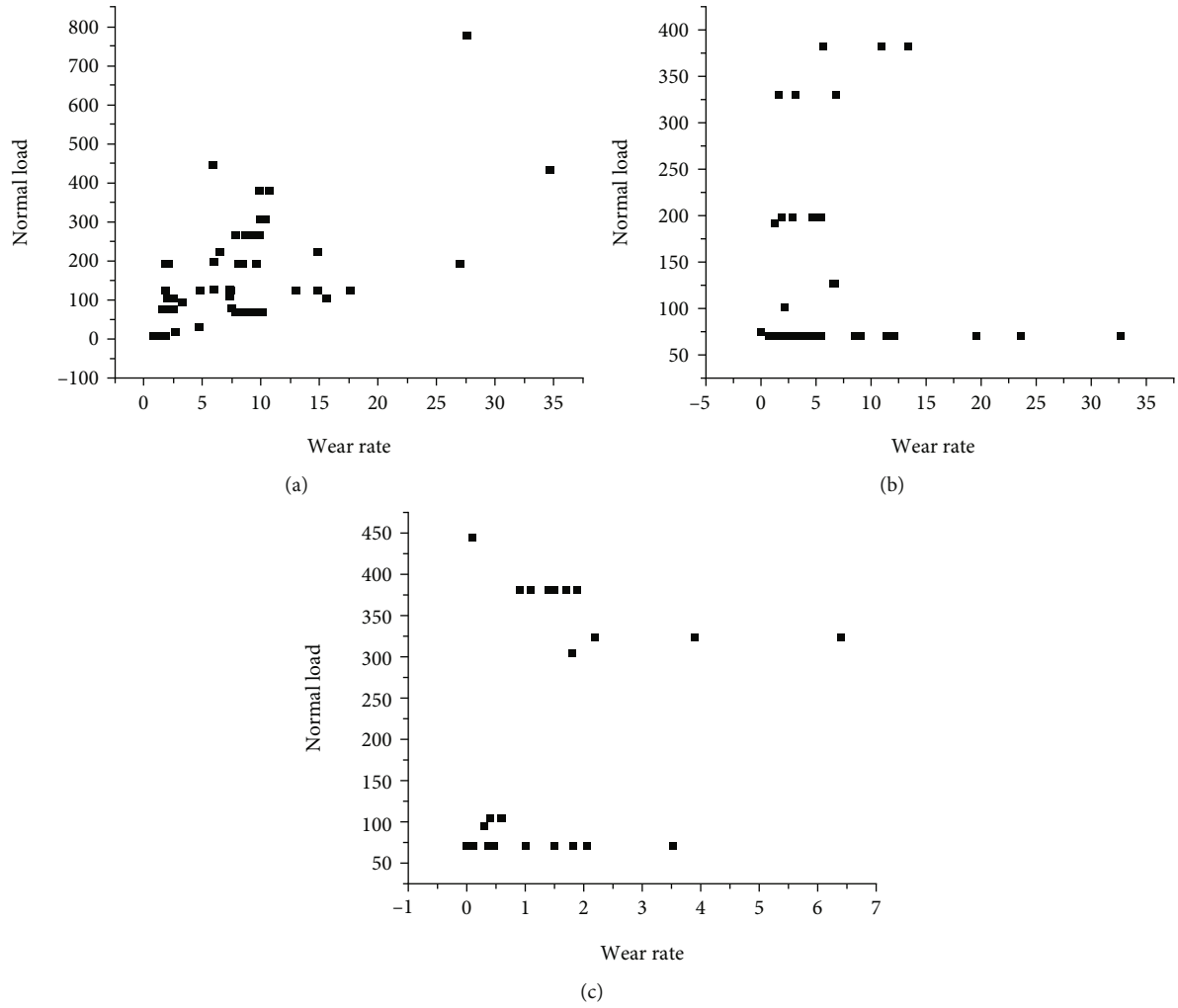

Figure 5: Scatter diagrams showing the effect of normal load on wear rates of UHMWPE. (a) 0 kGy (nonirradiated polyethylene), (b) 30-50 kGy (conventional polyethylene), and (c) 95-150 kGy (highly cross-linked UHMWPE-HXPE).

contact areas accompanied by a low radiation dose up to 40 kGy caused low wear rates of polyethylene.

The SHAP values for the average disc surface roughness R_a and its correlation with radiation doses were plotted in Figure 4(c). It was clear that the wear rates of polyethylene increased with R_a values higher than 0.05 μm, while it decreased below that value. Also, high radiation doses did not decrease the wear rate of UHMWPE with high values of surface roughness, which shows the significant impact of surface roughness on the wear rates. Persson et al. [65] reported that surface roughness affects the contact mechanisms and consequently has a big influence on the wear rate of articulating surfaces of hip and knee prosthesis.

Figure 4(d) showed the SHAP values for the sliding distance, where it was obvious that sliding distances of 30 mm/cycle had a high impact on the model's prediction for the wear rates of UHMWPE. This result shows that as the sliding distance increases above 30 mm per cycle associated with low values of loads up to 150 N, this leads to the increase in the wear rates of Polyethylene. The increase in the wear rates with increasing sliding distance per cycle was reported by McKellop et al. [66].

The dataset was further classified according to the radiation dose they received for sterilization and/or cross-linking in order to examine the effect of radiation doses on the wear rates of UHMWPE with different input operating parameters. The subgroups were as follows: 0 kGy (nonirradiated polyethylene), 30-50 kGy (conventional polyethylene), and 95-150 kGy (highly cross-linked UHMWPE-HXPE).

Scatter diagrams showing the effect of different operating parameters on the wear rates of UHMWPE were plotted in each subgroup and shown in Figures 5–8. Figure 5 shows scatter diagrams for the effect of normal load on the wear rates of UHMWPE in the three subgroups. It was noticed that at loads around 70 N, the wear rates were ranging between 1 and 10 mg/MC in the nonirradiated polyethylene while in the second subgroup (30-50 kGy), the wear rates were clustered in the range of 0-6 mg/MC and a few points were from 8 to 12 mg/MC. Wear rates of 0-2 mg/MC were obtained at the same load for the third subgroup (95-150 kGy). At higher loads above 200 N, there was an apparent difference between the nonirradiated and highly irradiated polyethylene (HXPE) where the wear rates of the nonirradiated polyethylene were in the range of 8-

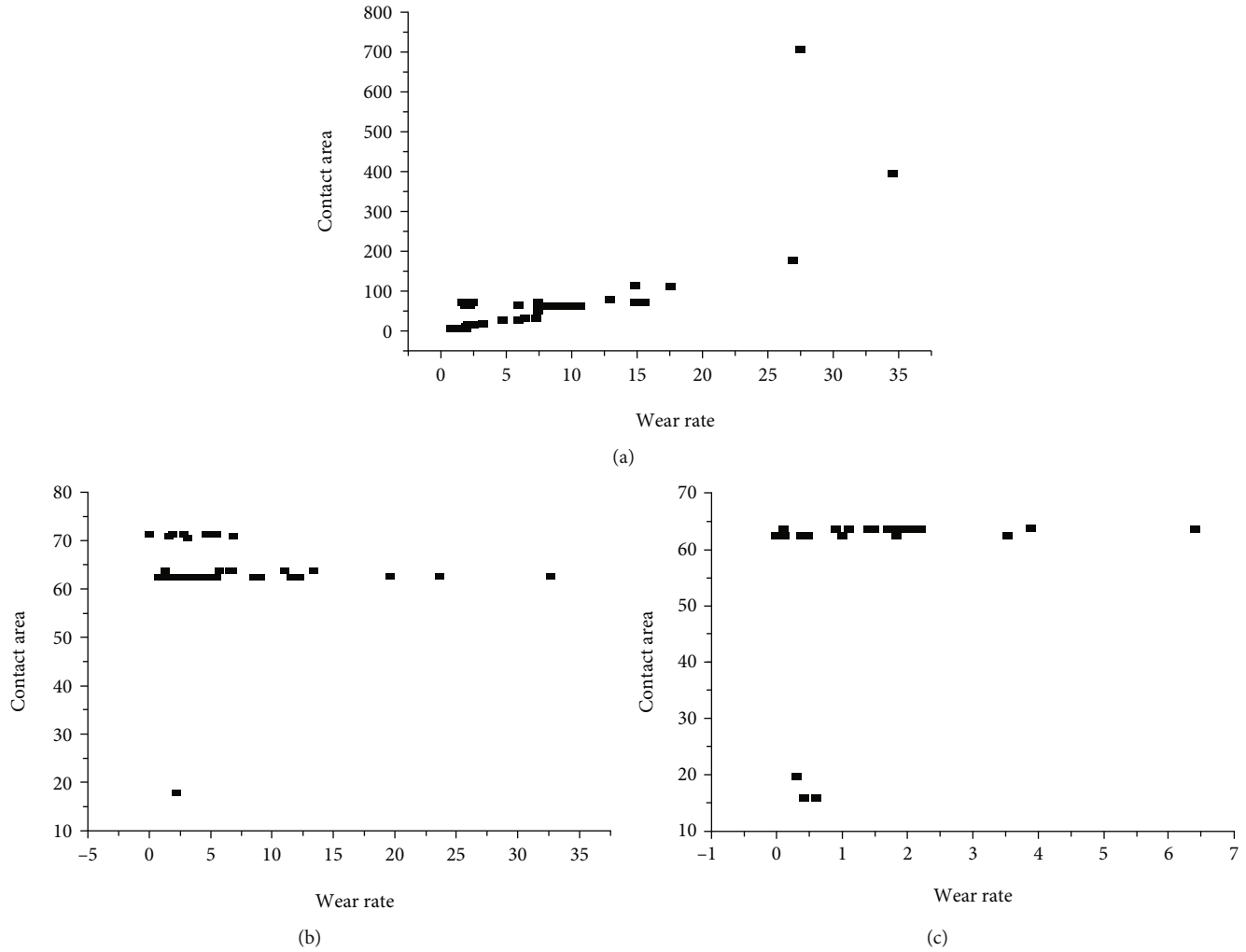

Figure 6: Scatter diagrams showing the effect of contact area on wear rates of UHMWPE. (a) 0 kGy (nonirradiated polyethylene), (b) 30-50 kGy (conventional polyethylene), and (c) 95-150 kGy (highly cross-linked UHMWPE-HXPE).

11 mg/MC and 1-2 mg/MC for HXPE. The variability of the wear results at the same load is due to the different operating test parameters. The clear difference in the wear rates shows the effect of radiation doses on the wear rates of UHMWPE where radiation doses higher than 95 kGy increased the wear resistance of UHMWPE, especially at high loads.

Furthermore, scatter diagrams showing the effect of contact area on the wear rates of UHMWPE were plotted in Figure 6. It was seen that the wear rates of the nonirradiated polyethylene increased with the increase of the contact area reaching 11 mg/MC at contact areas of approximately 64 mm^2 and continues to increase at higher contact areas. The wear rates for conventional polyethylene were ranging between 0 and 14 mg/MC at 64 mm^2 for different test parameters. The wear rates of the highly irradiated polyethylene (HXPE) were in the range 0-2 mg/MC at nearly the same contact area (around 64 mm^2).

Figure 7 reveals the impact of average disc surface roughness R_a on the wear rates of polyethylene in the three subgroups. At low values of R_a below 0.05 μm, it was seen that the wear rates of the nonirradiated polyethylene ranged nearly between 0 and 18 mg/MC and 0 and 8 mg/MC for conventional polyethylene. However, the highly irradiated UHMWPE (HXPE) produced a wear rate of 0 mg/MC for values of R_a below 0.05 μm and it increased to 2 mg/MC for R_a values above or equal 0.05 μm. This result reveals the pronounced effect of surface roughness and irradiation dose on the wear rates of polyethylene where R_a values below 0.05 μm and irradiation doses above 95 kGy produced 0 mg/MC wear rates. This finding confirms the results shown in the SHAP summary plot in Figure 4 where the irradiation dose and the average surface roughness were the top most significant factors having the highest impact on the model's prediction for wear rates of UHMWPE.

It was also clear from Figure 8 that HXPE had wear rates (0-2 mg/MC) at a sliding distance of 30 mm/cycle which are much lower than the nonirradiated and conventional polyethylenes. Despite the different test circumstances, highly cross-linked UHMWPE can be discriminated from conventional and nonirradiated UHMWPE based on wear rates.

Hence, the proposed model was able to predict the wear rates of UHMWPE based on different operating parameters

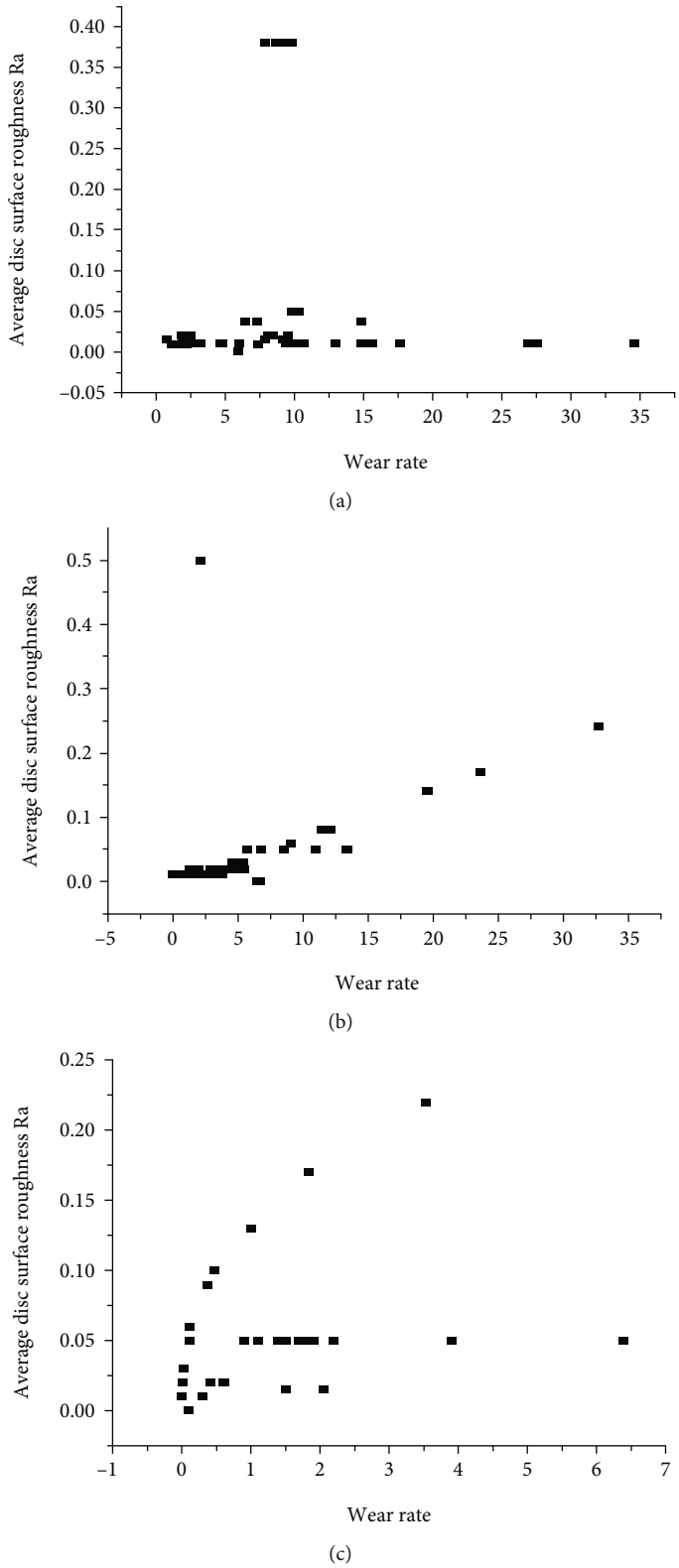

Figure 7: Scatter diagrams showing the effect of average disc surface roughness R_a on wear rates of UHMWPE. (a) 0 kGy (nonirradiated polyethylene), (b) 30-50 kGy (conventional polyethylene), and (c) 95-150 kGy (highly cross-linked UHMWPE-HXPE).

and it had the efficient capability to discriminate between different operating parameters and their effect on the wear rates and also prioritize the most important parameters that affect the model's prediction. This robust and efficient model can further help in visualizing other datasets and predicting the wear rates of polyethylene based on variable parameters

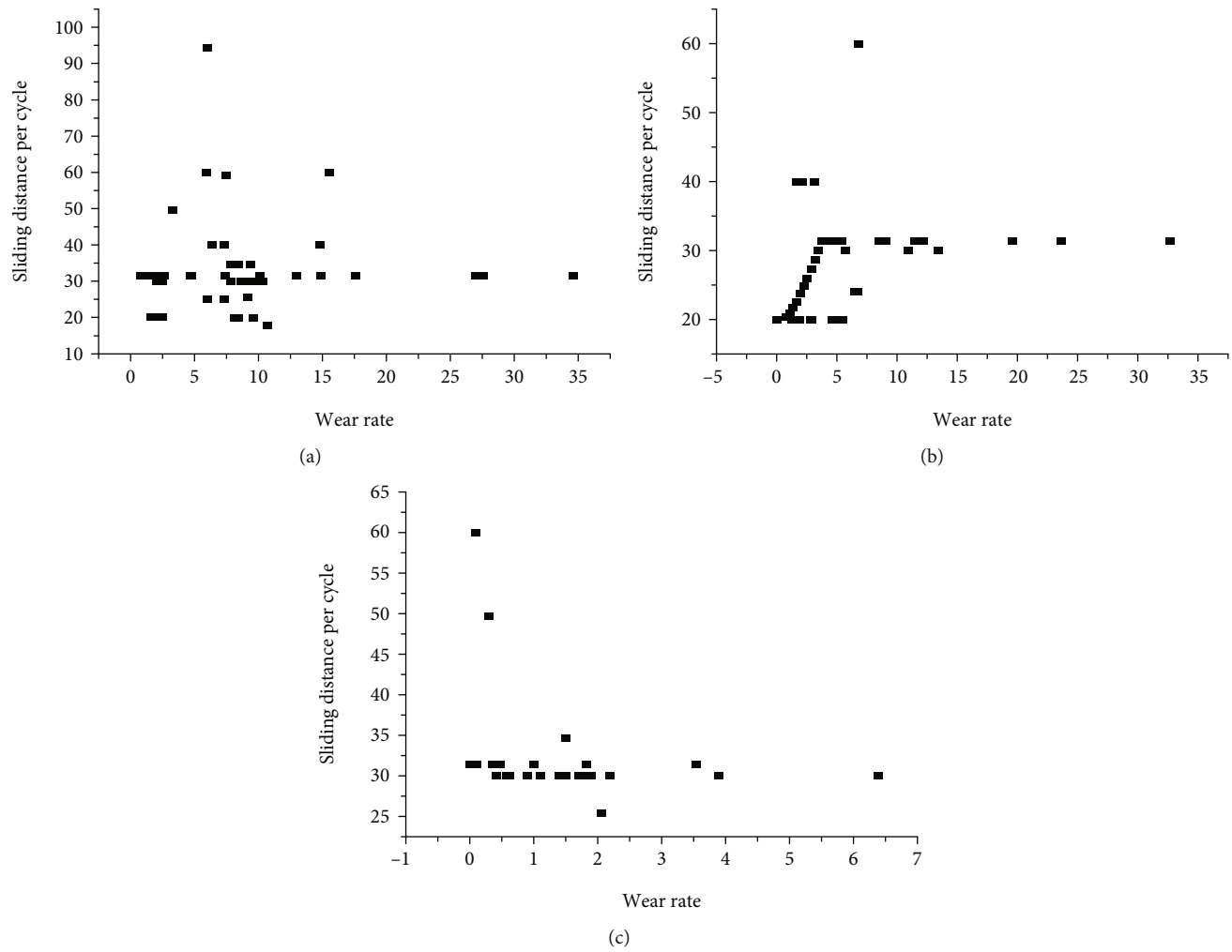

Figure 8: Scatter diagrams showing the effect of sliding distance on wear rates of UHMWPE. (a) 0 kGy (nonirradiated polyethylene), (b) 30-50 kGy (conventional polyethylene), and (c) 95-150 kGy (highly cross-linked UHMWPE-HXPE).

and hence deduce its behavior inside the human body and reduce the number of wear experiments. The model can also facilitate the design of UHMWPE-bearing materials with enhanced mechanical properties and design for applications in hip prosthesis.

Since the proposed study included only in vitro wear studies of polyethylene in PoD experiments, thus, future enhancement of the work includes further studies that should be conducted on the design of UHMWPE acetabular liners with improved mechanical properties utilized in metal-on-plastic hip implants. The liner should be made from highly cross-linked UHMWPE that is subjected to irradiation doses higher than 95 kGy which proved to have excellent wear resistance and its further implantation in the hip joints of clinically approved animals for in vivo long-term evaluation.

4. Conclusion

The primary aim of the proposed study is to develop a model having the highest efficiency and capability of predicting the wear rates of ultrahigh molecular weight polyethylene (UHMWPE), based on multidirectional motion in hip joint prosthesis and therefore help predict its in vivo wear behavior inside the body. The proposed machine learning model in this work is the support vector machine-grey wolf optimizer (SVM-GWO) hybrid regression system. For purpose of evaluation, the performance of the presented model was compared to other counterpart models including classic support vector machine (SVM), support vector machine using grey wolf optimizer (SVM-GWO), SVM using practical swarm optimizer (SVM-PSO), and SVM using genetic algorithm optimizer (SVM-GA). The results showed that the SVM-GWO outperformed the other implemented models since it attained the least root mean square error (RMSE) and the highest R^2 score for prediction of the wear rates of UHMWPE. Shapley additive explanations (SHAP) values were used to interpret the SVM-GWO model and to show the relative importance of the different variables (input operating parameters) on the predicted wear rates of UHMWPE.

The findings of this study revealed that the parameters having a significant effect on the model's prediction of UHMWPE wear rates are radiation doses, average disc surface roughness, contact area, normal load, and sliding

distance. Radiation doses had the maximum impact on the model's prediction, where high values of radiation doses had a negative impact on the model output (wear rate of UHMWPE) which implies that high doses of radiation decreased the wear rates of PE. The pronounced effect of surface roughness and irradiation doses on the wear rates of UHMWPE was seen in the results where R_a values below 0.05 μm and irradiation doses above 95 kGy produced 0 mg/MC wear rates. The high regression ability of the SVM-GWO model proves that it is a useful, efficient, and reliable model that can be utilized for the prediction of wear rates of UHMWPE bearings in hip joint prosthesis and aid in prioritizing the different variables that affect the wear rates of polyethylene.

The future work is directed to implement advanced technology to obtain better results, such as signal processing technology to improve the quality in the obtained results such as the technology proposed by the authors in [67–71].

Data Availability

The data that support the findings of this study are available from the corresponding author upon reasonable request.

Conflicts of Interest

The authors declare that they have no conflicts of interest.

References

[1] A. Wang and J. H. Dumbleton, "Ultra-high-molecular-weight polyethylene (UHMWPE) as a bearing material in hip joint replacements," in *Encyclopedia of Tribology*, pp. 3933–3939, Springer, MA, USA, 2013.

[2] H. P. Delport, S. A. Banks, J. De Schepper, and J. Bellemans, "A kinematic comparison of fixed-and mobile-bearing knee replacements," *Journal of Bone and Joint Surgery British Volume (London)*, vol. 88, no. 8, pp. 1016–1021, 2006.

[3] J. A. Williams, "Wear and wear particles–some fundamentals," *Tribology International*, vol. 38, no. 10, pp. 863–870, 2005.

[4] J. A. D'Antonio and K. Sutton, "Ceramic materials as bearing surfaces for total hip arthroplasty," *JAAOS-Journal of the American Academy of Orthopaedic Surgeons*, vol. 17, no. 2, pp. 63–68, 2009.

[5] S. M. Kurtz, O. K. Muratoglu, M. Evans, and A. A. Edidin, "Advances in the processing, sterilization, and crosslinking of ultra-high molecular weight polyethylene for total joint arthroplasty," *Biomaterials*, vol. 20, no. 18, pp. 1659–1688, 1999.

[6] S. Kavesh and D. C. Prevorsek, "Ultra high strength, high modulus polyethylene spectra fibers and composites," *International Journal of Polymeric Materials*, vol. 30, no. 1–2, pp. 15–56, 1995.

[7] J. Zeman, M. Ranuša, M. Vrbka, J. Gallo, I. Křupka, and M. Hartl, "UHMWPE acetabular cup creep deformation during the run-in phase of THA's life cycle," *Journal of the Mechanical Behavior of Biomedical Materials*, vol. 87, pp. 30–39, 2018.

[8] J. Zhou, A. Chakravartula, L. Pruitt, and K. Komvopoulos, "Tribological and nanomechanical properties of unmodified and crosslinked ultra-high molecular weight polyethylene for total joint replacements," *Journal of Tribology*, vol. 126, no. 2, pp. 386–394, 2004.

[9] R. K. Sethi, M. J. Neavyn, H. E. Rubash, and A. S. Shanbhag, "Macrophage response to cross-linked and conventional UHMWPE," *Biomaterials*, vol. 24, no. 15, pp. 2561–2573, 2003.

[10] Y. Di, X. Gang, and C. Chunhua, "The effect of gamma irradiation on the tribological properties of UHMWPE composite filled with HDPE," *Journal of Thermoplastic Composite Materials*, vol. 27, no. 8, pp. 1045–1053, 2014.

[11] J. Zhang, "Surface modification of ultra-high-molecular-weight polyethylene by argon plasma," *Journal of Thermoplastic Composite Materials*, vol. 27, no. 6, pp. 758–764, 2014.

[12] H. Liu, Y. Pei, D. Xie et al., "Surface modification of ultra-high molecular weight polyethylene (UHMWPE) by argon plasma," *Applied Surface Science*, vol. 256, no. 12, pp. 3941–3945, 2010.

[13] N. Chang, A. Bellare, R. E. Cohen, and M. Spector, "Wear behavior of bulk oriented and fiber reinforced UHMWPE," *Wear*, vol. 241, no. 1, pp. 109–117, 2000.

[14] S. Ge, S. Wang, and X. Huang, "Increasing the wear resistance of UHMWPE acetabular cups by adding natural biocompatible particles," *Wear*, vol. 267, no. 5–8, pp. 770–776, 2009.

[15] K. Plumlee and C. J. Schwartz, "Improved wear resistance of orthopaedic UHMWPE by reinforcement with zirconium particles," *Wear*, vol. 267, no. 5–8, pp. 710–717, 2009.

[16] S. Affatato, B. Bordini, C. Fagnano, P. Taddei, A. Tinti, and A. Toni, "Effects of the sterilisation method on the wear of UHMWPE acetabular cups tested in a hip joint simulator," *Biomaterials*, vol. 23, no. 6, pp. 1439–1446, 2002.

[17] M. S. Jahan, B. M. Walters, T. Riahinasab, R. Gnawali, D. Adhikari, and H. Trieu, "A comparative study of radiation effects in medical-grade polymers: UHMWPE, PCU and PEEK," *Radiation Physics and Chemistry*, vol. 118, pp. 96–101, 2016.

[18] R. Chiesa, M. C. Tanzi, S. Alfonsi, L. Paracchini, M. Moscatelli, and A. Cigada, "Enhanced wear performance of highly cross-linked UHMWPE for artificial joints," *Journal of Biomedical Materials Research: An Official Journal of The Society for Biomaterials, The Japanese Society for Biomaterials, and The Australian Society for Biomaterials and the Korean Society for Biomaterials*, vol. 50, no. 3, pp. 381–387, 2000.

[19] F. J. Medel and J. A. Puértolas, "Wear resistance of highly cross-linked and remelted polyethylenes after ion implantation and accelerated ageing," *Proceedings of the Institution of Mechanical Engineers, Part H: Journal of Engineering in Medicine*, vol. 222, no. 6, pp. 877–885, 2008.

[20] E. Oral, C. A. G. Beckos, A. J. Lozynsky, A. S. Malhi, and O. K. Muratoglu, "Improved resistance to wear and fatigue fracture in high pressure crystallized vitamin E-containing ultra-high molecular weight polyethylene," *Biomaterials*, vol. 30, no. 10, pp. 1870–1880, 2009.

[21] A. Wang, C. Stark, and J. H. Dumbleton, "Mechanistic and morphological origins of ultra-high molecular weight polyethylene wear debris in total joint replacement prostheses," *Proceedings of the Institution of Mechanical Engineers, Part H: Journal of Engineering in Medicine*, vol. 210, no. 3, pp. 141–155, 1996.

[22] K. L. K. Lim, Z. A. M. Ishak, U. S. Ishiaku et al., "High-density polyethylene/ultrahigh-molecular-weight polyethylene blend. I. The processing, thermal, and mechanical properties,"

Journal of Applied Polymer Science, vol. 97, no. 1, pp. 413–425, 2005.

[23] S. M. Kurtz, "Ultra high molecular weight polyethylene in total joint replacement and medical devices," in *UHMWPE Biomaterials Handbook*, Academic Press, New York, 2 edition, 2009.

[24] J. H. Dumbleton, A. Wang, K. Sutton, and M. T. Manley, *Highly Crosslinked and Annealed UHMWPE*, Elsevier, 2009.

[25] D. Baykal, R. S. Siskey, H. Haider, V. Saikko, T. Ahlroos, and S. M. Kurtz, "Advances in tribological testing of artificial joint biomaterials using multidirectional pin-on-disk testers," *Journal of the Mechanical Behavior of Biomedical Materials*, vol. 31, pp. 117–134, 2014.

[26] S. M. Kurtz, H. A. Gawel, and J. D. Patel, "History and systematic review of wear and osteolysis outcomes for first-generation highly crosslinked polyethylene," *Clinical Orthopaedics and Related Research*, vol. 469, no. 8, pp. 2262–2277, 2011.

[27] R. Ramprasad, R. Batra, G. Pilania, A. Mannodi-Kanakkithodi, and C. Kim, "Machine learning in materials informatics: recent applications and prospects," *npj Computational Materials*, vol. 3, no. 1, pp. 1–13, 2017.

[28] Y. Liu, Z. Song, X. Xu et al., "Bidirectional GRU networks-based next POI category prediction for healthcare," *International Journal of Intelligence Systems*, 2021.

[29] Y. Liu, A. Pei, F. Wang et al., "An attention-based category-aware GRU model for the next POI recommendation," *International Journal of Intelligence Systems*, vol. 36, no. 7, pp. 3174–3189, 2021.

[30] Y. Liu, D. Li, S. Wan et al., "A long short-term memory-based model for greenhouse climate prediction," *International Journal of Intelligence Systems*, vol. 37, no. 1, pp. 135–151, 2022.

[31] M. Abbasi and M. Rafiee, "A calibrated asymptotic framework for analyzing packet classification algorithms on GPUs," *The Journal of Supercomputing*, vol. 75, no. 10, pp. 6574–6611, 2019.

[32] I. Ahmed, Y. Zhang, G. Jeon, W. Lin, M. R. Khosravi, and L. Qi, "A blockchain-and artificial intelligence-enabled smart IoT framework for sustainable city," *International Journal of Intelligence Systems*, 2022.

[33] M. Abbasi, A. Najafi, M. Rafiee, M. R. Khosravi, V. G. Menon, and G. Muhammad, "Efficient flow processing in 5G-envisioned SDN-based internet of vehicles using GPUs," *IEEE Transactions on Intelligent Transportation Systems*, vol. 22, no. 8, pp. 5283–5292, 2021.

[34] A. Borjali, K. Monson, and B. Raeymaekers, "Predicting the polyethylene wear rate in pin-on-disc experiments in the context of prosthetic hip implants: deriving a data-driven model using machine learning methods," *Tribology International*, vol. 133, pp. 101–110, 2019.

[35] H. Haider and D. Baykal, "Wear assessment of UHMWPE with pin-on-disc testing," in *UHMWPE Biomaterials Handbook*, pp. 553–578, Elsevier, 2016.

[36] V. Saikko, O. Calonius, and J. Keränen, "Effect of counterface roughness on the wear of conventional and crosslinked ultra-high molecular weight polyethylene studied with a multi-directional motion pin-on-disk device," *Journal of Biomedical Materials Research: An Official Journal of The Society for Biomaterials, The Japanese Society for Biomaterials, and The Australian Society for Biomaterials and the Korean Society for Biomaterials*, vol. 57, no. 4, pp. 506–512, 2001.

[37] V. Saikko, "Effect of contact area on the wear and friction of UHMWPE in circular translation pin-on-disk tests," *Journal of Tribology*, vol. 139, no. 6, 2017.

[38] D. Mazzucco and M. Spector, "Effects of contact area and stress on the volumetric wear of ultrahigh molecular weight polyethylene," *Wear*, vol. 254, no. 5–6, pp. 514–522, 2003.

[39] J. G. Lancaster, D. Dowson, G. H. Isaac, and J. Fisher, "The wear of ultra-high molecular weight polyethylene sliding on metallic and ceramic counterfaces representative of current femoral surfaces in joint replacement," *Proceedings of the Institution of Mechanical Engineers, Part H: Journal of Engineering in Medicine*, vol. 211, no. 1, pp. 17–24, 1997.

[40] ASTM Committee F-4 on Medical and Surgical Materials and Devices, *Standard test method for wear testing of polymeric materials used in total joint prostheses*, ASTM International, 2011.

[41] E. Oral and O. K. Muratoglu, "Radiation cross-linking in ultra-high molecular weight polyethylene for orthopaedic applications," *Nuclear Instruments and Methods in Physics Research Section B: Beam Interactions with Materials and Atoms*, vol. 265, no. 1, pp. 18–22, 2007.

[42] J. A. K. Suykens and J. Vandewalle, "Least squares support vector machine classifiers," *Neural Processing Letters*, vol. 9, no. 3, pp. 293–300, 1999.

[43] M. A. Deif, M. A. A. Eldosoky, H. W. Gomma, A. M. El-Garhy, and A. S. Ell-Azab, "Adaptive neuro-fuzzy inference system controller technique for lower urinary tract system disorders," *Journal of Clinical Engineering*, vol. 40, no. 3, pp. 135–143, 2015.

[44] M. A. Deaf, M. A. A. Eldosoky, M. Ahmed, H. W. Gomma, and A. S. El-Azab, "Development of mathematical model for lower urinary tract dysfunctions," *Development*, vol. 2, no. 12, 2014.

[45] A. J. Kucharski, T. W. Russell, C. Diamond et al., "Early dynamics of transmission and control of COVID-19: a mathematical modelling study," *The lancet infectious diseases*, vol. 20, no. 5, pp. 553–558, 2020.

[46] H. Yan, J. Zhang, S. S. Rahman, N. Zhou, and Y. Suo, "Predicting permeability changes with injecting CO_2 in coal seams during CO_2 geological sequestration: a comparative study among six SVM-based hybrid models," *Science of the Total Environment*, vol. 705, article 135941, 2020.

[47] M. A. Deif, A. A. A. Solyman, M. H. Alsharif, and P. Uthansakul, "Automated triage system for intensive care admissions during the COVID-19 pandemic using hybrid XGBoost-AHP approach," *Sensors*, vol. 21, no. 19, p. 6379, 2021.

[48] M. Liu, Z. Cao, J. Zhang, L. Wang, C. Huang, and X. Luo, "Short-term wind speed forecasting based on the Jaya-SVM model," *International Journal of Electrical Power & Energy Systems*, vol. 121, article 106056, 2020.

[49] M. A. Deif, R. E. Hammam, and A. Solyman, "Gradient boosting machine based on PSO for prediction of leukemia after a breast cancer diagnosis," *International Journal on Advanced Science, Engineering and Information Technology*, vol. 11, no. 2, pp. 508–515, 2021.

[50] M. A. Deif, A. A. A. Solyman, M. H. Alsharif, S. Jung, and E. Hwang, "A hybrid multi-objective optimizer-based SVM model for enhancing numerical weather prediction: a study for the Seoul metropolitan area," *Sustainability*, vol. 14, no. 1, p. 296, 2022.

[51] S. Mirjalili, S. Saremi, S. M. Mirjalili, and L. S. Coelho, "Multi-objective grey wolf optimizer: a novel algorithm for multi-criterion optimization," *Expert Systems with Applications*, vol. 47, pp. 106–119, 2016.

[52] Q. Al-Tashi, H. M. Rais, S. J. Abdulkadir, S. Mirjalili, and H. Alhussian, "A review of grey wolf optimizer-based feature selection methods for classification," in *Evolutionary Machine Learning Techniques*, pp. 273–286, Springer, 2020.

[53] E. Akbari, A. Rahimnejad, and S. A. Gadsden, "A greedy non-hierarchical grey wolf optimizer for real-world optimization," *Electronics Letters*, vol. 57, no. 13, pp. 499–501, 2021.

[54] M. Deif, R. Hammam, and A. Solyman, "Adaptive neuro-fuzzy inference system (ANFIS) for rapid diagnosis of COVID-19 cases based on routine blood tests," *International Journal of Intelligent Systems*, vol. 14, no. 2, 2021.

[55] Z. Zhang and W.-C. Hong, "Application of variational mode decomposition and chaotic grey wolf optimizer with support vector regression for forecasting electric loads," *Knowledge-Based Systems*, vol. 228, article 107297, 2021.

[56] M. A. Deif and R. E. Hammam, "Skin lesions classification based on deep learning approach," *Journal of Clinical Engineering*, vol. 45, no. 3, pp. 155–161, 2020.

[57] M. A. Deif, A. A. A. Solyman, and R. E. Hammam, "ARIMA model estimation based on genetic algorithm for COVID-19 mortality rates," *International Journal of Information Technology & Decision Making*, vol. 20, no. 6, pp. 1775–1798, 2021.

[58] H. Lu, X. Ma, and M. Ma, "A hybrid multi-objective optimizer-based model for daily electricity demand prediction considering COVID-19," *Energy*, vol. 219, article 119568, 2021.

[59] L. S. Shapley, "A value for n-person games," in *Contributions to the Theory of Games*, vol. 2, pp. 307–317, Princeton University Press, Princeton, NJ, USA, 1953.

[60] M. A. Deif, R. E. Hammam, S. Ahmed, K. Mehrdad Ahmadi, S. B. Shahab, and E. H. Rania, "A deep bidirectional recurrent neural network for identification of SARS-CoV-2 from viral genome sequences," in *Mathematical Biosciences and Engineering*, vol. 18, no. 6pp. 8933–8950, AIMS–Press, 2021.

[61] R. Rodríguez-Pérez and J. Bajorath, "Interpretation of compound activity predictions from complex machine learning models using local approximations and Shapley values," *Journal of Medicinal Chemistry*, vol. 63, no. 16, pp. 8761–8777, 2020.

[62] S. C. Scholes and T. J. Joyce, "In vitro tests of substitute lubricants for wear testing orthopaedic biomaterials," *Proceedings of the Institution of Mechanical Engineers, Part H: Journal of Engineering in Medicine*, vol. 227, no. 6, pp. 693–703, 2013.

[63] Y. Sun, W. D. Zeng, X. M. Zhang, Y. Q. Zhao, X. Ma, and Y. F. Han, "Prediction of tensile property of hydrogenated Ti600 titanium alloy using artificial neural network," *Journal of Materials Engineering and Performance*, vol. 20, no. 3, pp. 335–340, 2011.

[64] O. K. Muratoglu, C. R. Bragdon, D. O. O'Connor et al., "Unified wear model for highly crosslinked ultra-high molecular weight polyethylenes (UHMWPE)," *Biomaterials*, vol. 20, no. 16, pp. 1463–1470, 1999.

[65] B. N. J. Persson, O. Albohr, U. Tartaglino, A. I. Volokitin, and E. Tosatti, "On the nature of surface roughness with application to contact mechanics, sealing, rubber friction and adhesion," *Journal of Physics. Condensed Matter*, vol. 17, no. 1, pp. R1–R62, 2005.

[66] H. McKellop, I. C. Clarke, K. L. Markolf, and H. C. Amstutz, "Wear characteristics of UHMW polyethylene: A method for accurately measuring extremely low wear rates," *Journal of Biomedical Materials Research*, vol. 12, no. 6, pp. 895–927, 1978.

[67] H. Attar, A. T. Abu-Jassar, V. Yevsieiev, V. Lyashenko, I. Nevliudov, and A. K. Luhach, "Zoomorphic mobile robot development for vertical movement based on the geometrical family caterplillar," *Computationa Intelligence and Neuroscience*, vol. 2022, article 3046116, 19 pages, 2022.

[68] H. H. Attar, A. A. A. Solyman, A.-E. F. Mohamed et al., "Efficient equalisers for OFDM and DFrFT-OCDM multicarrier systems in mobile E-health video broadcasting with machine learning perspectives," *Physical Communication*, vol. 42, p. 101173, 2020.

[69] A. Hani and K. R. Mohammad, "E-health communication system with multiservice data traffic evaluation based on a G/G/1 analysis method," *Therapy*, vol. 16, no. 2, pp. 115–121, 2021.

[70] A. A. Solyman, H. Attar, M. R. Khosravi, and B. Koyuncu, "MIMO-OFDM/OCDM low-complexity equalization under a doubly dispersive channel in wireless sensor networks," *International Journal of Distributed Sensor Networks*, vol. 16, no. 6, 2020.

[71] A. A. A. Solyman, H. Attar, M. R. Khosravi et al., "A low-complexity equalizer for video broadcasting in cyber-physical social systems through handheld mobile devices," *IEEE Access*, vol. 8, pp. 67591–67602, 2020.